Proceedings of IEEE-RAS International Conference on
Humanoid Robots (HUMANOIDS2001)
Tokyo, Japan, pp. 319–326, November 2001

Synthesis of a Walking Primitive Database for a Humanoid Robot using Optimal Control Techniques

J. Denk and G. Schmidt

Institute of Automatic Control Engineering,
Technische Universität München,
D-80290 Munich, Germany
Joachim.Denk@ei.tum.de, Guenther.Schmidt@ei.tum.de

Abstract

This paper presents a general method for generating walking primitives for anthropomorphic 3D–bipeds. Corresponding control torques allowing straight ahead walking with pre–swing, swing, and heel–contact are derived by dynamic optimization using a direct collocation approach. The computed torques minimize an energy based, mixed performance index. Zero moment point (ZMP) and friction conditions at the feet ensuring postural stability of the biped, as well as bounds on the joint angles and on the control torques, are treated as constraints. The method is applied to the model of a biped with 12 joints for the purpose of developing a walking primitive database allowing straight ahead walking with situation dependent step–length adaptation. The resulting biped motions are dynamically stable and the overall motion behaviour is remarkably close to that of humans.

Keywords

Humanoid Robot, Optimal Control, Walking Primitive Database, Step–Length Adaptation.

1 Introduction

Over the last years, major progress has been made in construction and stabilization of biped walking machines. Perception based goal–oriented autonomous walking, however, still remains an open field of research [1]. Locomotion in a partly unknown environment requires the ability of the biped to adapt its gait pattern according to the present situation, so that obstacles in the walking trail can be passed by or overcome. But, unlike industrial robots, bipeds are not fixed rigidly to the ground and have the tendency to tip over very easily. Their postural stability depends on the behaviour of six unpowered DOF defining their pose in the world, which can only be influenced indirectly by appropriate actuation of the powered DOF in the joints. Usually, the problem of executing a stable step–sequence is therefore solved by precomputation of an adequate reference trajectory, i.e., a walking pattern. As a consequence of the high nonlinearity and complexity of the system, however, it is not possible to achieve this in real time for a 3D biped in general. A possible solution is to compute a series of walking primitives for steps with different step parameters offline and to store them in a database. A situation dependent walking pattern can then be obtained by selection and concatenation of appropriate walking primitives during run–time.

Often, the problem of walking primitive synthesis is simplified by prescribing time trajectories for selected body parts [2–4]. These trajectories depend on the characteristics of the actual biped robot. The task of determining suitable trajectories relies on the designer's intuition and / or observations and biometric measurements of human gait behaviour. A method for walking primitive synthesis without any prescription of a priori knownledge about the motion has been reported in [5]. Dynamic optimization was applied to the model of a human body in order to find a repeatable movement minimizing metabolic energy per meter walked. The amount of supercomputer time needed, however, was excessive.

This paper deals with a general approach, which is suited for synthesizing databases of dynamically stable walking primitives [2] automatically in feasible time, by fusing the advantages of the methods mentioned earlier. To achieve this, first, the search space for a walking primitive is reduced by the general and reasonable assumption, that a walking primitive comprises the three gait phases pre–swing, swing and heel–contact and that one foot always remains flat on the ground while the other one is moving. Adequate motions are parameterized by the step parameters, i.e., step–length, step–width, and timing of the gait–phases. The search space is further confined to physically admissible trajectories. These trajectories satisfy the zero moment point (ZMP) [3] and friction conditions ensuring postural stability of the biped, conditions for smooth walking primitive concatenation and restrictions on joint angles and on the con-

trol torques given by the electrical and mechanical design. The remaining set of primitives is then searched for the walking primitive minimizing an energy based, mixed performance index using dynamic optimization. The corresponding optimal control problem is solved numerically by discretization of time using a direct–collocation approach [6]. Direct–collocation has already been applied successfully to synthesize walking primitives for a planar biped [7]; other examples of energy optimal planar walking are given in [8, 9].

The paper is structured as follows. The problem is formulated in Sec. 2 and the considered class of biped walking machines is defined. In Sec. 3 the search space for the optimization problem is characterized mathematically by specifying the properties of a walking primitive and the conditions for physical admissibility. After a discussion of the dynamic modelling approach used in Sec. 4, the optimal control problem is summerized in Sec. 5. We applied our approach as an example to the model of an anthropomorphic 3D–biped with 12 joints. A walking primitive database was generated allowing straight ahead walking with the step–lengths 0.30 m, 0.31 m, ..., 0.50 m. The necessary procedure and corresponding numerical results are presented in Sec. 6.

2 Problem Formulation

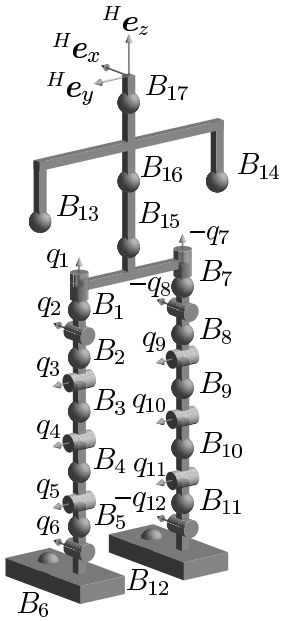

Figure 1: Kinematic scheme of biped robot with head frame H.

The described method is applicable to walking machines of the type illustrated in Fig. 1 consisting of bodies B_i, $i = 1 \dots N_b$ connected by driven joints with the joint angles and control torques q_i and τ_i, $i = 1 \dots N_j$ respectively. Symmetry of the biped's left and right side is assumed. The legs have to comprise at least six powered joints each, allowing to manipulate the feet in 6 DOF in Cartesian space relative to the torso. Further joints in the biped's torso are not considered in this work, but could be regarded in principle. The feet of the biped are assumed to be of such a kind, that the contact behaviour can be approximated by rigid body contacts, see Fig. 2.

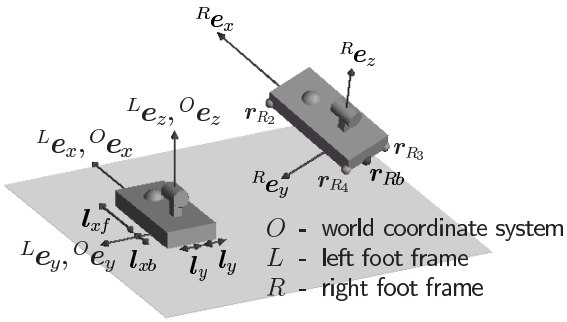

Figure 2: Biped feet with coordinate frames, lengths l, and points $\boldsymbol{r}$.

As input to the problem, the biped's kinematical parameters, all necessary dimensions, the masses and inertia tensors of the bodies B_i, the restrictions on joint angles q_i and joint velocities $\dot{q}_i$, the maximum allowed motor torques and the coefficients of friction between the feet and the ground have to be provided.

The joint angles are then subsumed in the vector $\boldsymbol{q} = [\boldsymbol{q}_l, \boldsymbol{q}_r]$, with the vectors $\boldsymbol{q}_l = [q_1 \dots q_{N_j/2}]^T$ and $\boldsymbol{q}_r = [q_{N_j/2+1} \dots q_{N_j}]^T$ representing the angles of the left and right leg respectively. Four coordinate systems are defined, the world coordinate system O, the head frame H and the contact frames L and R fixed in the sole of the left and right foot respectively. The pose of H, L and R with respect to O is given by $\boldsymbol{p}_H = [\boldsymbol{r}_H, \boldsymbol{\phi}_H]$, $\boldsymbol{p}_L = [\boldsymbol{r}_L, \boldsymbol{\phi}_L]$ and $\boldsymbol{p}_R = [\boldsymbol{r}_R, \boldsymbol{\phi}_R]$. The elements of vector $\boldsymbol{r} = [r_x \ r_y \ r_z]^T$ are Cartesian coordinates, $\boldsymbol{\phi} = [\phi_x \ \phi_y \ \phi_z]^T$ are orientations represented by roll–, pitch–, and yaw–angles. The posture of the biped is defined by the generalized coordinates $\boldsymbol{q}_g = [\boldsymbol{q}, \boldsymbol{p}_L]$.

The goal is now to synthesize a database of walking primitives allowing straight ahead walking with step–length adaptation. The individual primitives need to be computed in such a way, that they can be concatenated in realtime resulting in a smooth and physically feasible joint trajectory together with the corresponding control torques needed for driving the biped.

3 Walking Primitive

In the following subsections the search space of the optimal control problem is defined mathematically. First, the kinematics of a walking primitive are specified,

next, the conditions for contact stability are stated. Physical admissibility in addition requires that the joint angle and joint torque trajectories conform with restrictions given by the mechanical and electrical design. This problem is discussed in Sec. 3.3. Finally, conditions allowing the concatenation of individual walking primitives to a smooth trajectory are derived in Sec. 3.4.

3.1 Walking Primitive Kinematics

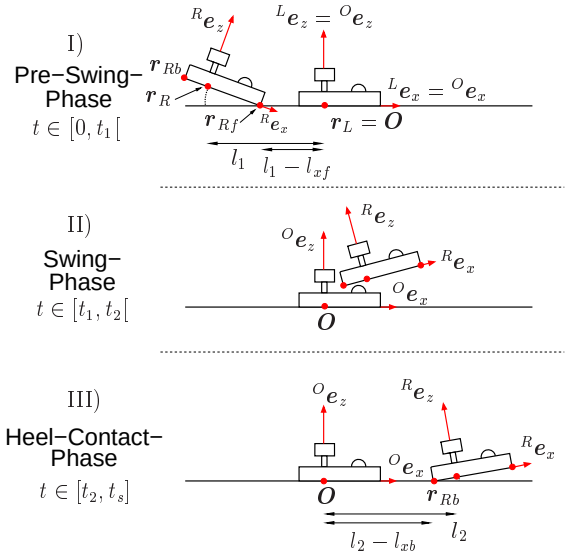

Figure 3: Three phases of walking primitive, side view.

The considered walking primitives comprise the 3 phases *pre–swing*, *swing* and *heel–contact* and represent a single step in the sagittal plane with the right foot swinging, see Fig. 3 and Fig. 4. The left foot resides flat on the ground in the origin of the world coordinate system O given by $\boldsymbol{p}_L(t) = \boldsymbol{0}$, $\forall t \in [0, t_s]$. With the transformation

$$\boldsymbol{q}_g(t) = \begin{bmatrix} \boldsymbol{q}(t) \\ \boldsymbol{p}_L(t) \end{bmatrix} = \begin{bmatrix} \boldsymbol{E} \\ \boldsymbol{0} \end{bmatrix} \boldsymbol{q}(t)\,, \forall t \in [0, t_s]\,,$$

where $\boldsymbol{E}$ is the identity matrix, the system can then be described in minimal coordinates $\boldsymbol{q}(t)$ for this contact situation reducing the number of system states during walking primitive synthesis from $2\times(N_j+6)$ to $2\times N_j$. In order to avoid undesirable mechanical stress, the trajectory $\boldsymbol{q}(t)$ is constrained to be continuous and continuously differentiable with respect to time. This implies that there are no jumps in the Cartesian velocities of the right foot and thus impacts are avoided when the heel contacts the ground.
During swing–phase the mechanism of the biped forms an open kinematic chain. During pre–swing and heel–contact, however, both feet contact the ground thus forming a closed chain. This is taken into account by kinematic constraints imposed on the system accelerations. These constraints and boundary conditions and inequality constraints necessary to characterize the kinematics of a walking primitive for the optimization process are summarized in the following. Step–length of the previous step l_1, step–length l_2, step width w, phase–transition–times t_1 and t_2 and step–duration t_s are used to parameterize the motion.

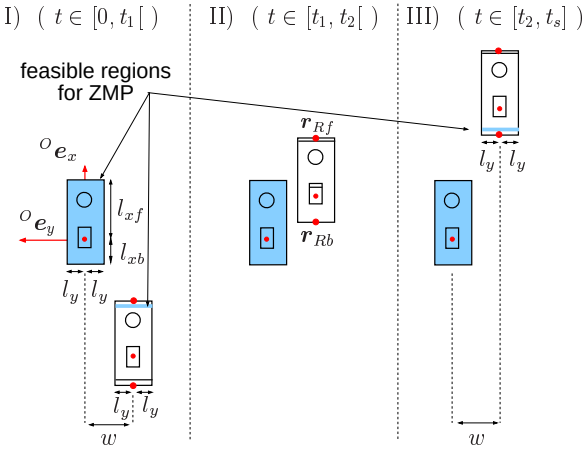

Figure 4: Three phases of walking primitive and feasible regions for ZMP, top view.

I) Pre–Swing–Phase ($t \in [0, t_1[$):
The walking primitive starts with the right foot located flat on the ground at $t = 0$. Pose and velocity are given by the boundary conditions

$$\begin{aligned} \boldsymbol{p}_R(0) &= \left[\begin{array}{ccc|ccc} -l_1 & -w & 0 & 0 & 0 & 0 \end{array}\right]^T \\ \begin{bmatrix} {}_O\dot{\boldsymbol{r}}_R(0) \\ {}_O\boldsymbol{\omega}_R(0) \end{bmatrix} &= \boldsymbol{C}_R(\boldsymbol{q}(0))\ \dot{\boldsymbol{q}}(0) = \boldsymbol{0}\,, \end{aligned} \tag{1}$$

where $\boldsymbol{C}_R$ is a Jacobian matrix, ${}_O\dot{\boldsymbol{r}}_R$ and ${}_O\boldsymbol{\omega}_R$ are the Cartesian and angular velocities represented in the world frame O. The respective initial system state is denoted $[\boldsymbol{q}_0\,,\ \dot{\boldsymbol{q}}_0] = [\boldsymbol{q}(0)\,,\ \dot{\boldsymbol{q}}(0)]$.
During $t \in]0, t_1[$, the right foot rolls over the toes. This contact situation is expressed by the kinematic constraint

$$\begin{bmatrix} {}_O\ddot{\boldsymbol{r}}_{Rf}(t) \\ {}_O\dot{\omega}_{R,x}(t) \\ {}_O\dot{\omega}_{R,z}(t) \end{bmatrix} = \boldsymbol{C}_{Rf}(\boldsymbol{q}(t))\ddot{\boldsymbol{q}}(t) + \dot{\boldsymbol{C}}_{Rf}(\boldsymbol{q}(t))\dot{\boldsymbol{q}}(t) = \boldsymbol{0} \tag{2}$$

The heel stays above ground which is ensured by the inequality constraint $r_{Rb,z}(t) \geq 0$.

II) Swing–Phase ($t \in [t_1, t_2[$):
The swing–phase starts with the right foot just about to

leave the ground at $t = t_1$ and then swinging towards its new position. External collisions with the ground and internal collisions with the left leg are avoided by use of the inequality constraints $r_{R_j,z}(t) \geq 0$, $j = 1 \ldots 4$, and $r_{R_j,y}(t) \leq -w_{min}$, $j = 2, 4$, with w_{min} representing a minimal lateral distance between the left and right leg.

III) Heel–Contact–Phase ($t \in [t_2, t_s]$):
At $t = t_2$ the foot touches the ground and rolls around the heel during $t \in]t_2, t_s[$. The corresponding kinematic constraint is given by

$$\begin{bmatrix} {}_O\ddot{\boldsymbol{r}}_{Rb}(t) \\ {}_O\dot{\omega}_{R,x}(t) \\ {}_O\dot{\omega}_{R,z}(t) \end{bmatrix} = \boldsymbol{C}_{Rb}(\boldsymbol{q}(t))\ddot{\boldsymbol{q}}(t) + \dot{\boldsymbol{C}}_{Rb}(\boldsymbol{q}(t))\dot{\boldsymbol{q}}(t) = \boldsymbol{0} \tag{3}$$

The toes need to remain above ground, which is ensured by $r_{Rf,z}(t) \geq 0$.
The walking primitive ends at $t = t_s$, when the right foot is flat on the ground again. Pose and velocity are given by the boundary conditions

$$\begin{aligned} \boldsymbol{p}_R(t_s) &= \left[\begin{array}{ccc|ccc} l_2 & -w & 0 & 0 & 0 & 0 \end{array}\right]^T \\ \begin{bmatrix} {}_O\dot{\boldsymbol{r}}_R(t_s) \\ {}_O\boldsymbol{\omega}_R(t_s) \end{bmatrix} &= \boldsymbol{C}_R(\boldsymbol{q}(t_s))\ \dot{\boldsymbol{q}}(t_s) = \boldsymbol{0}\ . \end{aligned} \tag{4}$$

The respective final system state is denoted by $[\boldsymbol{q}_s\ ,\ \dot{\boldsymbol{q}}_s] = [\boldsymbol{q}(t_s)\ ,\ \dot{\boldsymbol{q}}(t_s)]$.

3.2 Conditions for Contact Stability

An important feature of all forms of walking is, that physical contacts between a foot and the ground are unilateral. Stability of the contact situation during the three walking phases defined in Sec. 3.1 thus requires the occuring contact forces to conform with the contact stability conditions summarized next. The sum of all forces on a contact surface is thereby represented by the resultant contact forces $\boldsymbol{f} = [f_x\ f_y\ f_z]^T$ and moments $\boldsymbol{n} = [n_x\ n_y\ n_z]^T$ acting in the points $\boldsymbol{r}_L$, $\boldsymbol{r}_{Rf}$, $\boldsymbol{r}_{Rb}$ depending on the current walking phase, see Fig. 5.

• **Unilaterality Conditions** on the resultant normal contact forces ensure, that a desired contact situation does not change by a foot lifting off the ground:

$$\begin{aligned} f_{L,z} &\geq 0, \quad \forall t \in [0, t_s] \\ f_{Rf,z} &\geq 0, \quad \forall t \in [0, t_1[\\ f_{Rb,z} &\geq 0, \quad \forall t \in [t_2, t_s]\ . \end{aligned} \tag{5}$$

• **ZMP Conditions** [3] are used in this work to prevent a foot from beginning to rotate around its edges. The ZMP $\boldsymbol{r}_p$ is defined as the point on the contact surface, where the resultant moments n_x, n_y of all contact forces are zero. The contact situation is stable, if the ZMP remains inside the contact area.
With the resultant contact forces sketched in Fig. 5 the ZMP $\boldsymbol{r}_{pL}$ of the left foot, which should remain flat on the ground during all three phases, can be expressed in the left foot frame L as

$${}_Lr_{pL,x} = -\frac{n_{Ly}}{f_{Lz}} \quad , \quad {}_Lr_{pL,y} = \frac{n_{Lx}}{f_{Lz}}\ .$$

The following constraints result from the area of valid ZMP positions illustrated in Fig. 4 $\forall t \in [0, t_s]$:

$$-l_{xb} \leq -\frac{n_{Ly}}{f_{Lz}} \leq l_{xf}, \ -l_y \leq \frac{n_{Lx}}{f_{Lz}} \leq l_y\ . \tag{6}$$

As the right foot rotates around its front (back) edge during *pre–swing I* (*heel–contact III*) there is no resultant moment n_y and the contact surface degenerates to a line. The ZMP moves along this line while its coordinates in frame R are given by

$$\begin{aligned} {}_Rr_{pR,y} &= \frac{n_{Rf,x}}{f_{Rf,z}}\ , \quad {}_Rr_{pR,x} = l_{xf}\ , \quad \forall t \in [0, t_1[\\ {}_Rr_{pR,y} &= \frac{n_{Rb,x}}{f_{Rb,z}}\ , \quad {}_Rr_{pR,x} = -l_{xb}\ , \quad \forall t \in [t_2, t_s]\ . \end{aligned}$$

Considering the areas designated in Fig. 4 now leads to the constraints

$$\begin{aligned} -l_y \leq \frac{n_{Rf,x}}{f_{Rf,z}} \leq l_y, &\quad \forall t \in [0, t_1[\\ -l_y \leq \frac{n_{Rb,x}}{f_{Rb,z}} \leq l_y, &\quad \forall t \in [t_2, t_s] \end{aligned} \tag{7}$$

which ensure that the front (back) edge of the right foot remains flat on the ground.

• **Friction Conditions** ensure that a supporting foot neither begins to slip on the ground nor starts to rotate around the normal axis $\boldsymbol{e}_z$ of the contact surface. The resultant tangential forces f_x, f_y and the resultant moments n_z cannot be treated independently, because their effects combine. Thus the friction condition [2]

$$\sqrt{f_x^2 + f_y^2} + \left|\frac{n_z}{\kappa}\right| \leq \mu f_z \tag{8}$$

is applied, which has to be satisfied by the resultant contact forces $\boldsymbol{F}_L$ of the left foot during all three phases, by $\boldsymbol{F}_{Rf}$ at the right foot during *pre–swing I*, and by $\boldsymbol{F}_{Rb}$ during *heel–contact III*. The first term in (8) defines the usual friction cone, while the second is an additional tangential force induced by the moment n_z. The constant $0 < \mu < 1$ denotes the friction coefficient of the rubbing surfaces and κ is the frictional radius. The assumed frictional radius for the left foot is $\kappa_L = 0.5\sqrt{(2l_y)^2 + (l_{xb} + l_{xf})^2}$ and for the right foot $\kappa_{Rf} = \kappa_{Rb} = l_y$ during both pre–swing phase and heel–contact phase.

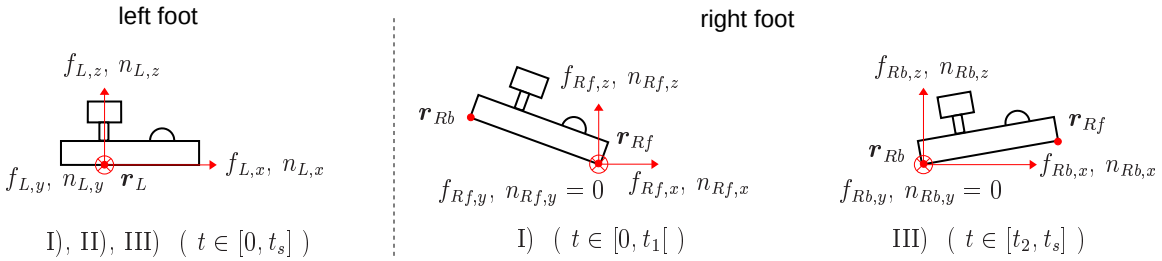

Figure 5: Contact constraints and forces during phases of walking primitive.

3.3 Mechanical and Electrical Restrictions

Physical admissibility of the walking primitives also demands compliance with restrictions given by the performance limits of the motors and by the mechanical mechanism. This is regarded by the inequality constraints

$$\begin{aligned} \boldsymbol{q}_{min} &\leq \boldsymbol{q}(t) \leq \boldsymbol{q}_{max} \\ \dot{\boldsymbol{q}}_{min} &\leq \dot{\boldsymbol{q}}(t) \leq \dot{\boldsymbol{q}}_{max}, \quad \forall t = [0, t_s]. \\ \boldsymbol{\tau}_{min} &\leq \boldsymbol{\tau}(t) \leq \boldsymbol{\tau}_{max} \end{aligned} \tag{9}$$

3.4 Conditions for Walking Primitive Concatenation

Step-length adaptation requires the concatenation of cyclic and transition walking primitives. These primitives are specified by additional constraints on the initial and final system states $[\boldsymbol{q}_0, \dot{\boldsymbol{q}}_0]$ and $[\boldsymbol{q}_s, \dot{\boldsymbol{q}}_s]$. For derivation of the related boundary conditions we will make use of the symmetry in the kinematic structure of the biped, allowing to easily obtain a walking primitive for the right foot supporting the biped, denoted by $\tilde{\boldsymbol{q}}(t)$, from the walking primitive $\boldsymbol{q}(t)$. It results by interchanging the joint angles of the left and right leg, which is performed by the mapping

$$\tilde{\boldsymbol{q}}(t) = [\boldsymbol{q}_r(t), \boldsymbol{q}_l(t)]\,, \quad t = [0, t_s]\,. \tag{10}$$

Respective joint torques $\boldsymbol{\tau}(t)$ are mapped accordingly. In order to obtain a cyclic walking primitive, the additional boundary conditions

$$\boldsymbol{q}_s = \tilde{\boldsymbol{q}}_0 \quad \text{and} \quad \dot{\boldsymbol{q}}_s = \dot{\tilde{\boldsymbol{q}}}_0 \tag{11}$$

are stated for a walking primitive with $l_1 = l_2 = a$. This allows the concatenation of $\boldsymbol{q}$ and $\tilde{\boldsymbol{q}}$ into a smooth walking pattern $\boldsymbol{q}$, $\tilde{\boldsymbol{q}}$, $\boldsymbol{q}$, $\tilde{\boldsymbol{q}}$, $\boldsymbol{q}$, ... enabling continuous symmetric cyclic walking with a given step–length a, see also [1]. A cyclic walking primitive is denoted by $\boldsymbol{q}^{l_1 \rightsquigarrow l_2} = \boldsymbol{q}^{a \rightsquigarrow a}$ in the following.

For concatenation of two cyclic walking primitives $\boldsymbol{q}^{a \rightsquigarrow a}$ and $\boldsymbol{q}^{b \rightsquigarrow b}$ with different step–lengths $a \neq b$, see Fig. 6, a transition walking primitive $\boldsymbol{q}^{a \rightsquigarrow b}$ is defined. In order to obtain a continuous state trajectory after concatenation, initial and final states of the transition primitive have to match the corresponding states of the cyclic primitives. This is ensured by the boundary conditions

$$\begin{aligned} \boldsymbol{q}_0^{a \rightsquigarrow b} &= \tilde{\boldsymbol{q}}_s^{a \rightsquigarrow a} \quad \text{and} \quad \dot{\boldsymbol{q}}_0^{a \rightsquigarrow b} = \dot{\tilde{\boldsymbol{q}}}_s^{a \rightsquigarrow a}, \\ \boldsymbol{q}_s^{a \rightsquigarrow b} &= \tilde{\boldsymbol{q}}_0^{b \rightsquigarrow b} \quad \text{and} \quad \dot{\boldsymbol{q}}_s^{a \rightsquigarrow b} = \dot{\tilde{\boldsymbol{q}}}_0^{b \rightsquigarrow b}. \end{aligned} \tag{12}$$

When the transition primitive is mapped according to (10) the primitive $\tilde{\boldsymbol{q}}^{a \rightsquigarrow b}$ shown in the center of Fig. 6 is obtained. This primitive can then be concatenated with the two cyclic primitives yielding the complete transition as depicted in Fig. 6 on the right. The resulting walking pattern enables the biped to execute three steps with the step–lengths a, b and b.

In order to enable walking with n different step–lengths, a database of n cyclic walking primitives with different step–lengths $l = l_1 = l_2$ needs to be computed. Considering possible transitions between all of the cyclic primitives $p = n(n-1)$ transition primitives are required.

4 Dynamic Modeling

The system dynamics in the three phases are modeled under the assumption of bilateral rigid body contacts between the feet and the ground. This allows the exertion of contact forces in all directions contrary to physical reality. In combination with the contact stability conditions formulated in Sec. 3.2, however, the modeling is permissible, because they prevent the occurrence of contact forces not being compatible with the actual unilateral contact situation.

The dynamics of the biped in minimal coordinates $\boldsymbol{q}(t) \in \mathbb{R}^{N_j}$ are then given by

$$\boldsymbol{M}\ddot{\boldsymbol{q}} = \boldsymbol{h} + \boldsymbol{\tau} + \boldsymbol{C}_{Rf}^T \boldsymbol{F}_{Rf} + \boldsymbol{C}_{Rb}^T \boldsymbol{F}_{Rb} \tag{13}$$

with $\boldsymbol{M}(\boldsymbol{q})$ the mass–matrix, $\boldsymbol{h}(\boldsymbol{q}, \dot{\boldsymbol{q}})$ coriolis, centrifugal, and gravity effects, and $\boldsymbol{\tau}$ the joint torques. The Jacobians $\boldsymbol{C}_{Rf}(\boldsymbol{q}) \in \mathbb{R}^{5 \times N_j}$ and $\boldsymbol{C}_{Rb}(\boldsymbol{q}) \in \mathbb{R}^{5 \times N_j}$ obtained in (2) and (3) are projecting the generalized constraint contact forces $\boldsymbol{F}_{Rb} = [\boldsymbol{f}_{Rb}, n_{Rb,x}, n_{Rb,z}] \in \mathbb{R}^{5 \times 1}$ and $\boldsymbol{F}_{Rf} = [\boldsymbol{f}_{Rf}, n_{Rf,x}, n_{Rf,z}] \in \mathbb{R}^{5 \times 1}$ on the generalized coordinates. Since the contact situation of the left foot is formulated in minimal coordinates, the forces $\boldsymbol{F}_L = [\boldsymbol{f}_L, \boldsymbol{n}_L] \in \mathbb{R}^{6 \times 1}$ are not part of the dynamic system

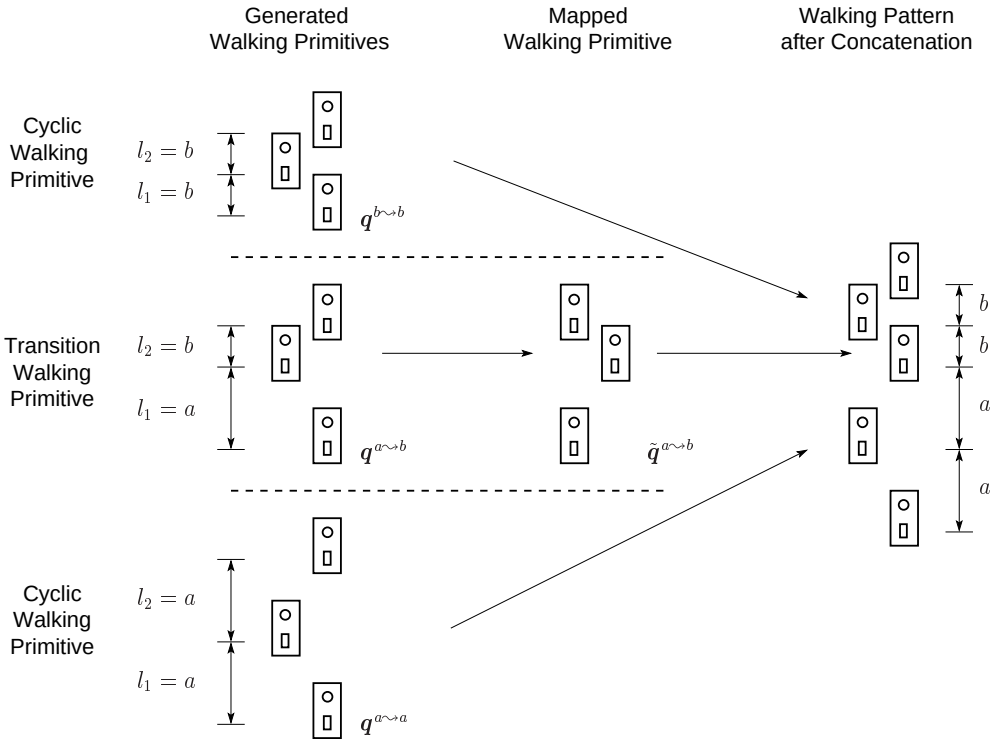

Figure 6: Changing step–lengths by a transition primitive.

equations. However, they can be recalculated easily using the Principle of D'Alambert as soon as $\ddot{\boldsymbol{q}}$ and the external forces on the right foot have been determined, see also [2]. The system accelerations during *swing–phase II* ($\boldsymbol{F}_{Rb} = \boldsymbol{F}_{Rf} = \boldsymbol{0}$) are computed as

$$\ddot{\boldsymbol{q}} = \boldsymbol{M}^{-1}(\boldsymbol{h} + \boldsymbol{\tau}) \ , \ \forall t \in [t_1, t_2[\, . \tag{14}$$

During *pre–swing I* ($\boldsymbol{F}_{Rb} = \boldsymbol{0}$) resp. *heel–contact III* ($\boldsymbol{F}_{Rf} = \boldsymbol{0}$) the 5 additional equations (2) resp. (3) on the system accelerations are used together with (13) to solve for $[\ddot{\boldsymbol{q}}, \boldsymbol{F}_{Rf}]$ resp. $[\ddot{\boldsymbol{q}}, \boldsymbol{F}_{Rb}]$ resulting in:

$$\begin{aligned} \ddot{\boldsymbol{q}} =& \boldsymbol{M}^{-1}(\boldsymbol{h} + \boldsymbol{\tau} + \boldsymbol{C}_{Rf/b}^T \boldsymbol{F}_{Rf/b}) \\ \boldsymbol{F}_{Rf/b} =& -(\boldsymbol{C}_{Rf/b}\boldsymbol{M}^{-1}\boldsymbol{C}_{Rf/b}^T)^{-1} \\ & (\boldsymbol{C}_{Rf/b}\boldsymbol{M}^{-1}(\boldsymbol{h} + \boldsymbol{\tau}) + \dot{\boldsymbol{C}}_{Rf/b}\dot{\boldsymbol{q}}) \\ & \forall t \in [0, t_1[\ / \ [t_2, t_s] \, . \end{aligned} \tag{15}$$

5 Optimal Control Problem

The instantaneous mechanical power P_i transmitted by a motor in the i-th joint of the biped is given as $P_i(t) = \dot{q}_i(t)\tau_i(t)$, with τ_i the motor torque. The energy released by the system when backdriving the motor ($P_i(t) < 0$) is usually not used for recharging the power source. This is regarded in the performance index by penalizing the sum of the absolute values of $P_i(t)$, $i = 1 \ldots N_j$, indicating, that power is actively consumed when dissipating this energy [8]. However, a performance index solely based on the minimization of $|P_i(t)|$, results in a motion with the right foot swinging very closely to the ground. This is an undesirable effect for execution of the trajectories on a physical biped. We therefore introduce an additional term during swing–phase, which penalizes the right foot being too close to the ground, cf. Fig. 2:

$$\begin{aligned} \min_{\boldsymbol{\tau}(t)} \Bigg(& \int_0^{t_1} \sum_{i=1}^{N_j} \left| \frac{P_i(t)}{P_n} \right| dt \\ & + \int_{t_1}^{t_2} \sum_{i=1}^{N_j} \left| \frac{P_i(t)}{P_n} \right| + \sum_{j=1}^{4} e^{\alpha(\epsilon - r_{R_{j,z}})} dt \\ & + \int_{t_2}^{t_s} \sum_{i=1}^{N_j} \left| \frac{P_i(t)}{P_n} \right| dt \Bigg) \end{aligned} \tag{16}$$

with t_1,t_2 and t_s given and fixed; P_n, α and ϵ are constant parameters.
This functional needs to be minimized subject to:

(i) the differential equations (14), (15) of the system according to the actual motion phase
(ii) the contact stability conditions (5), (6), (7), (8)
(iii) the inequality constraints for collision avoidance
(iv) phase connection conditions on the system state at $t = t_1$ and $t = t_2$ ensuring a continuous state trajectory

(v) the inequality constraints on the joint angles, joint velocities and joint torques to satisfy restrictions given by the mechanical and electrical design (9)

(vi) the boundary conditions (1) and (11) for a cyclic primitive or (12) for a transition primitive

6 Numerical Results

The described method was applied to a simplified model of the biped robot "Johnnie" developed at TU München [10]. Its kinematics is illustrated in Fig. 1. Three joints are located in each hip, one joint in the knees and two joints in the ankles. Numerical results for a sample walking primitive database allowing straight ahead walking with the step–lengths 0.30 m, 0.31 m, ..., 0.5 m are presented next.

The database was obtained by solving the optimal control problems stated in Sec. 5 for the necessary 441 cyclic and transition walking primitives with the direct–collocation software DIRCOL [6]. DIRCOL converts the continuous optimal control problem into a static optimization problem by discretization of trajectories in time. The resulting nonlinear programming problem is then solved by the sparse solver SNOPT [11]. All necessary dynamical equations were derived with the help of AUTOLEV [12], a tool for analytical motion analysis.

The ratio of phase–transition–time t_1 to step duration $p_1 = t_1/t_s = 0.12$, the ratio of phase–transition–time t_2 to step duration $p_2 = t_2/t_s = 0.93$ and the average forward velocity $v = (l_1 + l_2)/(2t_s) = 0.71$ m/s were assumed as fixed, allowing t_1, t_2 and t_s to be determined from l_1 and l_2. Although optimal control theory as well as DIRCOL allow for treating the temporal parameters t_1 and t_2 as additional optimization variables they are considered here as fixed for purposes of improved convergence. The step–width used was $w = 0.20$ m, the friction coefficient $\mu = 0.7$ and the parameters in the performance function $P_n = 1$ W, $\alpha = 300$ /m and $\epsilon = 0.01$ m.

Using a trajectory for statically stable walking [1] as a rough initial solution, a cyclic walking primitive $\boldsymbol{q}^{0.3\rightsquigarrow 0.3}$ was generated by subsequent refinement of the discretization and by gradually adding the constraints. The computation time required thereby strongly depended on the quality of the initial solution and on the fineness of the discretization. Typically, a solution could be obtained within a few hours using a current standard PC and about 20 grid points. The resulting trajectories for the position of the biped's center of mass (COM) in the world–coordinate system O and the orientation of the head frame given by RPY–angles $\boldsymbol{\phi}_H$ are depicted in Fig. 7. The relatively large oscillation in the pitch angle $\phi_{H,z}$ are due to a missing degree of freedom around the z-axis in the torso of the biped and the fact, that the left foot resides flat on the ground. The amplitudes further increase for longer step–lengths.

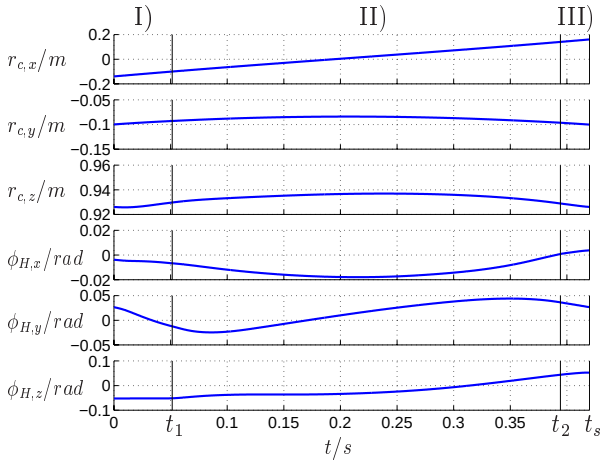

Figure 7: Resulting trajectories for position $\boldsymbol{r}_c$ of COM and orientation $\boldsymbol{\phi}_H$ of biped head for cyclic walking primitive with $l = l_1 = l_2 = 0.3$ m.

Beginning with the initial solution $\boldsymbol{q}^{0.3\rightsquigarrow 0.3}$ previously obtained, the optimization runs for walking primitive database synthesis were started. For all optimizations, 20 grid points were used. First, cyclic walking primitives were computed by an automatic procedure systematically increasing the step–length by $\Delta l = 0.01$ m and starting the optimizations using the feasible trajectory of the previous optimization run as an initial guess. This strategy takes advantage of the fact, that convergence is greatly enhanced in the vicinity of existing solutions. By this procedure, the cyclic walking primitives with $l = 0.31$ m, 0.32 m, ..., 0.50 m could be obtained within 2 hours computation time, with all but one primitive converging without user intervention.

Subsequently, the optimizations for the $n = 21 \times 20 = 420$ transition primitives $\boldsymbol{q}^{a\rightsquigarrow b}$ were started. The necessary final and initial system states, cf. (12), were read from the respective cyclic primitives $\boldsymbol{q}^{a\rightsquigarrow a}$ and $\boldsymbol{q}^{b\rightsquigarrow b}$ automatically. The cyclic primitives $\boldsymbol{q}^{a\rightsquigarrow a}$ also served as starting trajectory to each problem. The computation time needed was 6 days on a single computer, although distribution of the optimizations to different computers is possible. 94% of the optimization problems converged without user intervention.

The motion of the head, center of mass and feet in the x-z-plane after concatenation of cyclic and transition walking primitives to a walking pattern with the step–lengths $l = 0.35$ m, 0.41 m, 0.30 m, 0.50 m, 0.50 m are shown in Fig. 8.

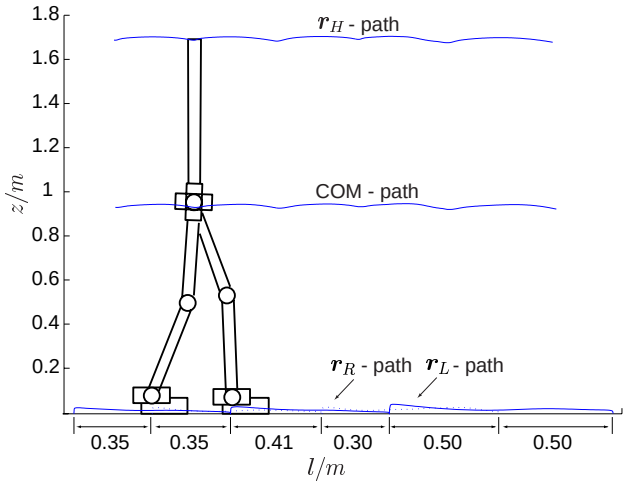

Figure 8: Path of head, COM and feet in the sagittal plane for a step sequence with the step–lengths $l = 0.35$ m, 0.41 m, 0.30 m, 0.50 m, 0.50 m .

7 Conclusions and Future Work

The results presented in this paper demonstrate that dynamically stable, physically feasible, and naturally looking walking primitives can be generated by optimal control techniques using direct collocation methods. This approach is well suited for automatically generating databases of primitives by systematic variation of the walking parameters, because convergence is greatly enhanced in the vicinity of existing solutions. Future work will consider curve walking and striding over obstacles in addition to straight ahead walking. The resulting database will then be used to provide the walking patterns required for perception–based adaptive walking of a biped robot [1].

Acknowledgments

This work was supported in part by the German Research Foundation (DFG) within the "Autonomous Walking" Priority Research Program. The authors thank U. Hanebeck for valuable comments. We would also like to express our gratitude to O. von Stryk and P. E. Gill for making their programs DIRCOL and SNOPT available for this research.

References

[1] O. Lorch, J. Denk, J. F. Seara, M. Buss, F. Freyberger, and G. Schmidt, "ViGWaM — An Emulation Environment for a Vision Guided Virtual Walking Machine," in *Proceedings of the IEEE/RAS International Conference on Humanoid Robots (Humanoids)*, (Cambridge, Massachusetts, USA), September 2000.

[2] C. L. Shih et al, "Trajectory Synthesis and Physical Admissibility for a Biped Robot During the Single-Support Phase," in *Proceedings of the IEEE International Conference on Robotics and Automation*, (Cincinnati, Ohio), pp. 1646–1652, 1990.

[3] M. Vukobratović, B. Borovac, D. Surla, and D. Stokić, *Biped Locomotion*, vol. 7 of *Scientific Fundamentals of Robotics*. Berlin, Germany: Springer–Verlag, 1 ed., 1990.

[4] K. Nagasaka, H. Inoue, and M. Inaba, "Dynamic Walking Pattern Generation for a Humanoid Robot Based on Optimal Gradient Method," in *Proceedings of the IEEE International Conference on Systems, Man and Cybernetics*, (Tokyo, Japan), pp. 908–913, 1999.

[5] M. G. Pandy and F. C. Anderson, "Dynamic Simulation of Human Movement using Large–Scale Models of the Body," in *Proceedings of the IEEE International Conference on Robotics and Automation*, (San Francisco, California), pp. 676–681, 2000.

[6] O. von Stryk, *User's Guide for DIRCOL: A Direct Collocation Method for the Numerical Solution of Optimal Control Problems*. Lehrstuhl für Höhere Mathematik und Numerische Mathematik, Technische Universität, München, 2.1 ed., 1999.

[7] M. Hardt, J. Helton, and K. Kreutz-Delgado, "Optimal Biped Walking with a Complete Dynamical Model," in *Proceedings of the 38th IEEE Conference on Decision and Control*, (Phoenix, AZ), pp. 2999–3004, December 1999.

[8] P. Channon, S. Hopkins, and D. Pham, "Derivation of optimal walking motions for a bipedal walking robot," *Robotica*, vol. 10, pp. 165–172, 1992.

[9] C. Chevallereau and Y. Aoustin, "Optimal reference trajectories for walking and running of a biped robot," *Robotica*, vol. 19, pp. 557–569, 2001.

[10] M. Gienger, K. Loeffler, and F. Pfeiffer, "Towards the Design of a Biped Jogging Robot," in *Proceedings of the IEEE International Conference on Robotics and Automation*, (Seoul, Korea), pp. 4140–4145, 2001.

[11] P. E. Gill, W. Murray, and M. A. Saunders, *User's Guide for SNOPT 5.3: A Fortran Package for Large-Scale Nonlinear Programming*. Department of Mathematics, University of California, San Diego, 2.1 ed., 1999.

[12] T. R. Kane and D. A. Levinson, *DYNAMICS ONLINE*. OnLine Dynamics, Inc., Sunnyvale, USA, 1996.